

# MODEL-BASED CLUSTERING OF DIGITAL PCR DROPLETS USING EXPECTATION MAXIMIZATION

A Thesis Proposal  
Presented to  
the Faculty of the College of Science  
De La Salle University Manila

In Partial Fulfillment  
of the Requirements for the Degree of  
Master of Science in Statistics

by

GUIAO, Joyce Emlyn B.

Frumencio F. Co  
Adviser

April 13, 2020

## **Abstract**

From 150 to 200 words of short, direct and complete sentences, the abstract should be informative enough to serve as a substitute for reading the thesis document itself. It states the rationale and the objectives of the research.

In the final thesis document (i.e., the document you'll submit for your final thesis defense), the abstract should also contain a description of your research results, findings, and contribution(s).

Keywords can be found at <http://www.acm.org/about/class/class/2012?pageIndex=0>. Click the link "HTML" in the paragraph that starts with "The full CCS classification tree...".

**Keywords:** Keyword 1, keyword 2, keyword 3, keyword 4, etc.

# Contents

<b>1</b>	<b>Research Description</b>	<b>1</b>
1.1	Introduction . . . . .	1
1.2	Background of the Study . . . . .	1
1.3	Statement of the Problem . . . . .	5
1.4	Significance of the Study . . . . .	5
1.5	Scope and Limitations . . . . .	6
<b>2</b>	<b>Review of Related Literature</b>	<b>7</b>
2.1	dPCR Droplet Classification Methods . . . . .	7
2.1.1	Droplet dPCR (ddPCR) System . . . . .	7
2.1.2	Manual Global Threshold (MTg) . . . . .	9
2.1.3	Kernel Density Estimation (KDE) . . . . .	9
2.1.4	K-Nearest-Neighbors (KNN) . . . . .	11
2.1.5	Model-Based Clustering . . . . .	13
2.2	Expectation-Maximization (EM) Clustering . . . . .	15
<b>3</b>	<b>Theoretical Framework</b>	<b>16</b>
3.1	EM Clustering . . . . .	16

3.1.1	Model-based clustering . . . . .	16
3.1.2	G-component Finite Mixture Density . . . . .	16
3.1.3	Expectation Maximization . . . . .	16
3.2	Performance Evaluation . . . . .	16
<b>4</b>	<b>Methodology</b>	<b>17</b>
4.1	Data . . . . .	18
4.1.1	Rain Experiment Dataset . . . . .	18
4.1.2	DNA Quantification Dataset . . . . .	18
4.2	Model Fitting and Classification . . . . .	18
4.3	Performance Evaluation . . . . .	18
<b>A</b>	<b>Diagrams and Other Documentation Tools</b>	<b>19</b>
<b>B</b>	<b>Theoretical and/or Conceptual Framework</b>	<b>20</b>
<b>C</b>	<b>Resource Persons</b>	<b>21</b>
	<b>References</b>	<b>22</b>

# List of Figures

1.1	The dPCR workflow . . . . .	2
1.2	Potential variation components between steps of the dPCR workflow	2
1.3	Fluorescence readings of 4 repetitions of DNA target cru . . . . .	4
1.4	Fluorescence readings of 4 repetitions of DNA target TC1507 . . .	4
2.1	QuantaSoft threshold from a study . . . . .	8
2.2	Fluorescence distribution of DNA target acp . . . . .	11
2.3	Determined thresholds calculated by definetherain . . . . .	12

# List of Tables

# Chapter 1

## Research Description

### 1.1 Introduction

### 1.2 Background of the Study

Quantification of Nucleic acids (NA) is a developing research field in molecular biology for the detection and quantification expression levels of genes (Huggett, O’Grady, & Bustin, 2015). These NA molecules are found in deoxyribonucleic acid (DNA) and ribonucleic acid (RNA), which carries genetic information and is used as biomarkers for the detection of diseases (?, ?). Additionally, along with the rise of bioinformatics tools, NA quantification methods are also utilized in rare mutation detection, copy number variation detection, single-cell gene and microRNA expression analysis, and next-generation sequencing (Quan, Sauzade, & Brouzes, 2018). Outside the scope of molecular biology, its application has also found its way in forensic research (Whale, Cowen, Foy, & Huggett, 2013), medical diagnosis, environmental monitoring, and food safety analysis (?, ?).

To be able to determine the concentration of target NAs, NA detection is naturally a pre-requisite. There are, however, NAs of interests that have very low concentrations to the point that it becomes undetectable in existing detection technologies. This problem is solved by amplifying the NA sequences using Polymerase Chain Reaction (PCR), a widely-used method for NA amplification since its invention in the 1980s (?, ?). PCR can multiply specific NA sequences in DNA or RNA from low concentrations to millions of copies. This method exposes the NA sequences mixed with chemical components in a series of 20 to 40 temperature cycles. In each cycle, PCR doubles the NA molecule; theoretically producing  $2^n$

molecules after  $n$  cycles (Quan et al., 2018).

After PCR amplification, absolute NA quantification is achieved using digital Polymerase Chain Reaction (dPCR) technique. This equally divides the NA samples into thousands of partitions; each of these partitions is evaluated as either off or on, or in this context, labeled as positive or negative, hence the term "digital" (?. ?).

The dPCR workflow, as illustrated in Figure 1.1, is usually a sequential procedure of extracting the sample from an organism, concocting the sample with several chemical components into a reaction mix, distributing the reaction mix to equal partitions, amplifying and detecting the target molecules using PCR, and the concentration is then finally estimated using a Poisson correction factor. In (Jacobs, Goetghebeur, & Clement, 2014), it was emphasized that every step of the dPCR workflow inevitably allows for the introduction of different sources of variation. These variance components within the dPCR workflow is shown in Figure 1.2.

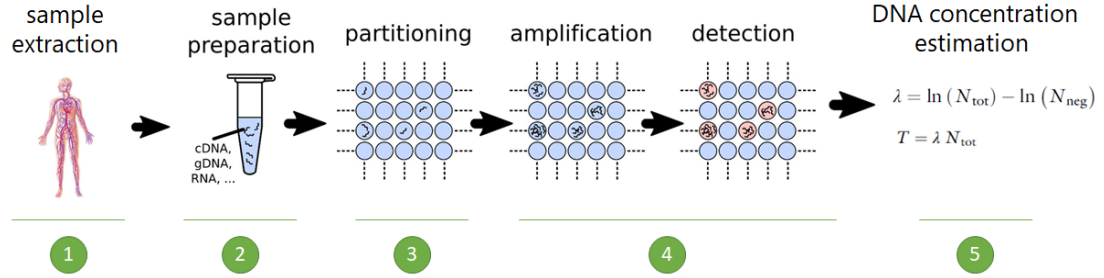


Figure 1.1: The dPCR workflow

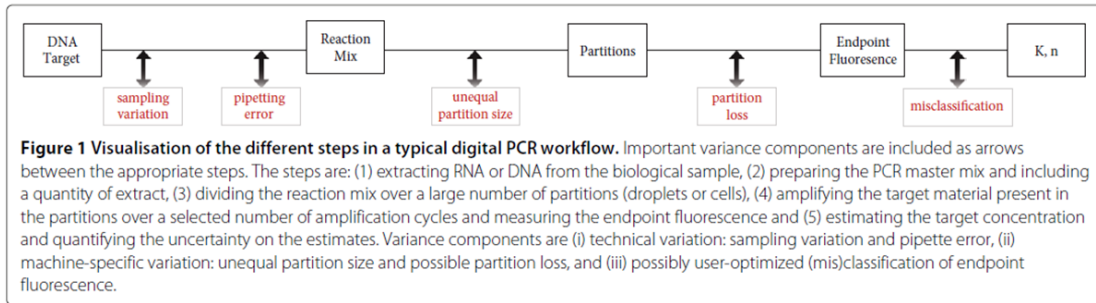


Figure 1.2: Potential variation components between steps of the dPCR workflow

Sampling variation stems from the fact that only a small sample of the organism is extracted; and although there is an expected number of target molecules per liters of a sample, drawing equally sized samples will result in different target molecules that are more or less near the average. Tzonev (n.d.) demonstrates the



number of target molecules that can be drawn from extraction is distributed as Poisson. Besides the sampling error, samples may also exhibit imperfections, and thus have inhibited amplification.

Preparing the reaction mix is a delicate process that strictly requires the accuracy of the pipetting volume; and yet, technical variation still occurs that results in pipetting errors. The next variation components are the possibility of the distributed partitions to be of unequal volumes and the loss of partitions due to physical interventions. Finally, upon PCR amplification, each droplet partition emits an endpoint fluorescence that would be used to classify the partition as positive or negative. However, some partitions are difficult to classify due to inhibition, delayed reactions, primer depletion, and other biological factors.

Each variance component accumulates to the bias and variance of the final estimated target molecule concentration, and thus, this gives rise to the importance of providing solutions that would increase precision in every step. To increase the sensitivity and specificity of the estimate, the misclassification of droplet partition should be minimized as much as possible. A high presence of false-negative droplets reduces sensitivity, while specificity is lowered for high false-positive count. Due to the variance contributed by misclassification, Tzonev (n.d.) recommends reporting the rates of false positives (FPR) and false negatives (FPN) per partition. More importance is given to either of the two depending on the kind of test being performed. If the total negative partition is expected to be large, then there is more chance that a true negative partition may turn into a false positive reading; which in this case, FPR may be of more interest than FNR.

The primary problem in misclassification lies in 'rain' droplets; these are partitions that emits an intermediate fluorescence signal that is difficult to classify as positive or negative. Figures 1.3 and 1.4 demonstrates two different DNA targets with the former showing a visually clearer distinction of the positive and negative population than the latter, of which is possessing multiple rain droplets. The data used in these figures are sourced from the publicly available dataset from the study of Lievens et al. (2016).

The estimate for DNA target concentration highly depends on the positive and negative classifications. For experiments with low copy DNA targets, the focus is on maximizing the sensitivity of the test for these very small number of positive droplets. Low sensitivity translates to failure in detecting lower concentrations.

For assays with large differences in the distance between the two fluorescence groups (positive and negative droplets), most quantification tools estimate the target concentrations with high sensitivity. As exhibited in an optimized assay experiment of *E. amylovora* (Dreo et al., 2014), slight differences of thresholds



Figure 1.3: Fluorescence readings of 4 repetitions of DNA target cru

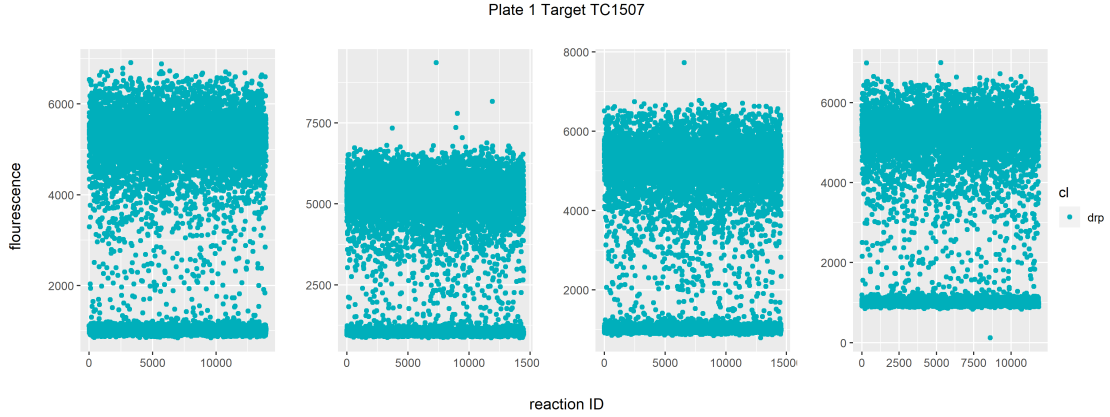


Figure 1.4: Fluorescence readings of 4 repetitions of DNA target TC1507

calculated from different tools had little effect on the final estimated concentration. However, for *R. solanacearum*, which is observed to manifest false-positive signals in qPCR experiments, produces unsatisfactory analytical sensitivity of the concentration estimates.

The danger of false rates due to misclassification is expounded at the clinical level, where false rates lead to the misdiagnosis of patients (Tzonev, n.d.). One such case is the prenatal screening test for Down Syndrome; this test is expected to mostly result in normal pregnancies. However, even for a small FPR, many pregnancies are still falsely reported as positive for Down Syndrome. False negatives also risk the overall health of the patient that truly possesses the genetic disorder.

## 1.3 Statement of the Problem

This thesis aims to classify dPCR droplet partitions into positive or negative by exploring Model-Based clustering with Expectation Maximization. The specific objectives of this study are to:

1. Fit two-component finite mixture densities on the datasets with varying amounts of rain and increasing target DNA concentration;
2. Classify partitions using the fitted models for each experiment and estimate DNA concentration using the standard formula;
3. Evaluate and compare the precision and bias of the estimates amongst the existing classification methods.

## 1.4 Significance of the Study

Quantification of target concentrations for pathogenic bacteria, gene expression of diseases, cancer diagnostic, and other health-related applications strongly demand estimators with high sensitivity and precision, as lives are put to risk for false-positives. A modern approach to DNA and RNA target quantification is through the dPCR method. In one of the steps of the dPCR workflow, the classification of droplet fluorescence still has areas of improvement.

The most prominent problem in classification lies in experiments exhibiting a high frequency of rain, or intermediate fluorescence values. These are experiments that have not yet been optimized. As different DNA target samples exhibit distinct structures (Lievens et al., 2016), an optimized setup for one DNA target may not be applicable for other targets. Additionally, for samples with low concentration, the total count of detected positive droplets dramatically changes the final concentration estimate, due to the greater impact of false positives in the proportion of detected over the number of true positives. The following are some tools and methodologies proposed for droplet classification: Quantasoft propriety software, definetherain (Jones et al., 2014a), manual global threshold (Dreo et al., 2014), cloudy (Lievens et al., 2016), and Umbrella (Jacobs et al., 2017). Most of the aforementioned droplet classifying tools rely strongly on how representative reference samples are. According to Dreo et al. (2014), such approaches are sensitive to significant shifts in amplitude for previously unobserved factors, such as cross-reactions or the influence of inhibitors.

In an attempt to prevent the problem of representation, this study will explore the feasibility of estimating target concentrations without a reference sample. Similar to Umbrella, this study also aims to use model-based clustering for the droplet classification but with relaxing the assumptions using the Expectation-Maximization algorithm. The significance of the study will be useful in quantifying concentrations in targets that have not yet been optimized for dPCR experiments and also for quantifying targets of low concentrations.

## 1.5 Scope and Limitations

This study solely relied on publicly available fluorescence datasets from published research papers. Only two were found and will be used for statistical analysis, namely from Lievens et al. (2016) and Jones et al. (2014a). The former dataset contains twelve DNA targets from food and feed samples ran on nine different settings by controlling for experimental factors; the latter dataset is a serial dilution of the Albumin DNA ranging from  $10^0$  to  $10^5$  copies.

The droplet classification method in this study uses model-based clustering, or the use of finite mixture models to perform clustering. However, the identification of the distribution of the mixture densities will be dependent on the observed available dataset. As a consequence of the limited dataset, the paper’s methodology described here needs more study for other experimental setting and nucleic acid targets.

Lastly, statistical results presented may lack biological explanations which could be useful for explaining the variances of the droplet fluorescence. Such information may be utilized to further improve the estimation process.

# Chapter 2

## Review of Related Literature

### 2.1 dPCR Droplet Classification Methods

#### 2.1.1 Droplet dPCR (ddPCR) System

The most common method in classifying positive and negative droplets is by enforcing a hard threshold. Generally, all droplets with a fluorescence amplitude greater than this threshold are then classified as positive, and negative otherwise.

One popular tool incorporated with automatic thresholding is the QuantaSoft software. The QuantaSoft software is the dPCR analysis tool that comes with the Bio-Rad droplet dPCR (ddPCR) System package. It allows for the setting up of sample and experiments, running and controlling the instrument, and finally, the analysis of the NA concentration (Bio-Rad, 2019). According to the Bio-Rad Laboratories website (<https://www.bio-rad.com>), it has been a leading product developer for 65 years in the research fields of life science and clinical diagnostics. Among its popular focus areas, dPCR is one of its most featured technology, providing ddPCR instruments; kits, reagents and assays; and other consumables. Several studies in hospitals (López et al., 2016; D. F. Chen, Zhang, Tan, & Jing, 2018; Abed, Carbonneau, L’Huillier, Kaiser, & Boivin, 2017; Tagliapietra et al., 2020), public health (Hussain & Bowers, 2017a; Nystrand, Ghanima, Waage, & Jonassen, 2018), food safety (J. Chen et al., 2020; Capobianco et al., 2020; Basanisi et al., 2020), upto environmental quality (Hamaguchi et al., 2018; Jahne et al., 2020; Dobnik, Štebih, Blejec, Morisset, & Žel, 2016; Mauvisseu et al., 2019) have found the Bio-Rad QuantaSoft dPCR systems useful for their analyses.

Of all the QuantaSoft software features, the focus of this section is on its threshold setting. By default, QuantaSoft sets an automatic threshold to the single-well or multiple-well amplitude data; a demonstration is shown in Figure 2.1. As with other automated tools, its documentation recommends reviewing this threshold to make changes if needed; and thus, manually setting the threshold is also allowed. Unfortunately, the calculation of the automatic threshold is not publicly available.

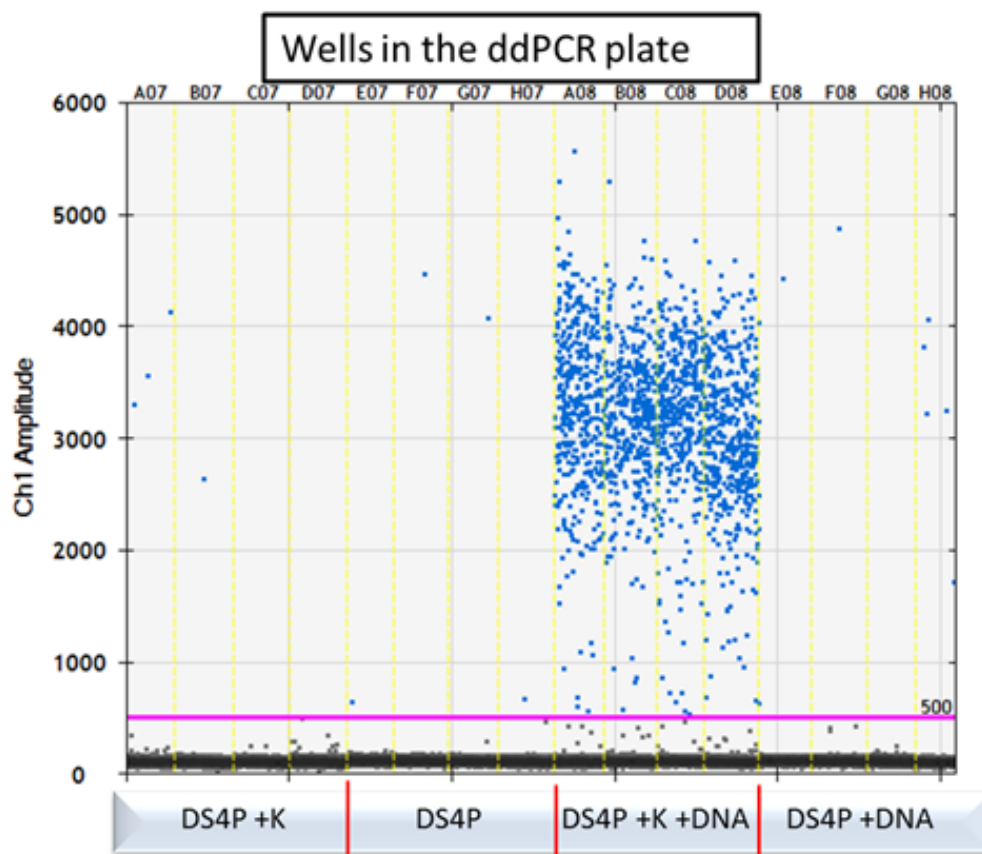


Figure 2.1: QuantaSoft threshold in pink line from (Hussain & Bowers, 2017b)

The evaluation of the QuantaSoft software show exemplary results from the food safety study of Basanisi et al. (2020), whereby nine pure meat samples were discriminated with 100% diagnostic accuracy, sensitivity, and specificity. However, upon checking the authenticity of twenty commercially available meat products, twelve samples were said to contain DNA traces of other animals not declared. Among the several reasons for this high detection, Basanisi et al. (2020) suggests the need for a highly sensitive and specific test in the molecular level. Observation of NA molecules can be done through their droplet fluorescence in a dPCR assay.

Assessing the QuantaSoft software’s ability to classify droplets, it was shown that for samples exhibiting a substantial amount of intermediate fluorescence, the system fails to determine a threshold (outputs ”No call”). This was the case in the two bacteria study of (Dreo et al., 2014), that were ran on very high concentrations. In the case of low bacteria concentrations, droplets near the negative droplets were classified as positives. This study concluded that the QuantaSoft software requires a well-optimized assay with good discrimination of positive and negative droplets for its threshold to be reliable.

### 2.1.2 Manual Global Threshold (MTg)

As opposed to the automatic threshold, Dreo et al. (2014) proposes setting a manual global threshold (MTg) determined by no template control (NTC) samples. This takes into consideration that individual assays behave differently, and could require expert intervention. For example, the threshold for a well-optimised assay was defined as the NTC mean + 6 standard deviations; on the other hand, a noisy assay had its threshold set above the highest value in NTC samples. It is expected in the latter example that the sensitivity would be lower, due to its high threshold. However, the paper claims that this resulted in high analytical sensitivity for that assay. A major disadvantage in this approach is the clear definition or guidelines in setting the MTg; this consequently will cause reproducibility issues for succeeding experiments and external researchers.

### 2.1.3 Kernel Density Estimation (KDE)

The positive and negative droplet classification can be framed as a clustering problem. One solution is by using the popular theory of kernel density estimation (KDE); whereby each data point influence is modeled using a kernel function — frequently Gaussian distributed, and the sum of all the kernel functions would be the overall density of the data. Clusters can then be derived from the estimated densities depending on its application (Hinneburg & Keim, 2003).

KDE has been particularly helpful in spatial analysis. Clusters were detected in areas with diabetes in Berlin (Kauhl, Schweikart, Krafft, Keste, & Moskwyn, 2016), HCV hepatitis C virus in Massachusetts (Stopka et al., 2017), and crime hotspots in Brazil (Junior, Da Silva, De Queiroz Neto, De MacÊdo, & Porcino, 2019). For other data types, KDE clustering has been improved in an algorithm developed by Rodriguez and Laio (2014), called clustering by fast search and find of density peaks. This technique has piqued the interests of many researchers;

thereby further improving the original limitations via DNA genetic algorithm (Zang, Ren, Zhang, & Liu, 2017), heat diffusion (Mehmood, Zhang, Bie, Dawood, & Ahmad, 2016), and entropy of data field (Wang, Wang, Li, Li, & Ding, 2016).

Although not named in the dPCR optimization paper of Lievens et al. (2016), cloudy is the name of the function in their supplementary source code file that calculates the threshold from the clusters found by using Gaussian KDE. The following steps explain this in more detail:

1. Estimate the density function of the fluorescence using a Gaussian kernel density with a minimum bandwidth of 50
2. Identify density peaks using a sliding window approach. The subsequent steps will differ according to if one, two, or more than three peaks were found. But generally, the proceeding steps are followed.
3. For each population found through the peaks, its location and spread is initially estimated using the median  $\hat{\mu}$  and  $\hat{\sigma}$ . Assuming normality, the latter is estimated as half the peak width at 60-65% of its maximum height.
4. Refine the estimates using a reiterative method, first initialized with  $a = 4$ .
5. Re-estimate  $\hat{\mu}$  and  $\hat{\sigma}$  using only the observations within  $\hat{\mu} \pm (a \cdot \hat{\sigma})$ .
6. Recalculate  $a = 4.55 + 0.35 \cdot \log(k) + 0.045 \cdot \log(k)^2$ ; where  $k$  is the kurtosis of the distribution
7. Repeat steps 5-6 until stabilization.
8. After stabilizing the estimates for all the population, the last step is different when either including or excluding rain in the final categorization.
  - (a) If rain is included as a category, observations within  $\hat{\mu} \pm (a \cdot \hat{\sigma})$  are then classified as members of that population; observations not falling within any population are classified as rain.
  - (b) If rain categorization is not of interest, then a threshold  $\theta = \hat{\mu}_n + 1.5 \cdot a_n + \hat{\sigma}_n$  is calculated; where  $n$  is a population.

In summary, the cloudy algorithm uses the Gaussian kernel density and normality assumptions to detect peaks, which are then considered as populations. From then population density parameters are estimated based on specified formulas. A range or a single threshold is then calculated for classifying droplets as positive, negative, or optionally, rain.



Special cases such as overlapping population boundaries and threshold placement problems are also checked in their source code. It is worth noting that in step 6, the formula for re-calculating  $a$  for density parameter estimation is based on the analysis of their in-house data, and should be used with caution when implementing for other unobserved NA targets. The rain classification rule in step 8(a) also poses a problem for fluorescence densities that are heavily skewed. Figure 2.2 left panel reveals the distribution of negative droplets to be heavily skewed to the right, thereby causing their exclusion to be labeled as negative due to the symmetry of the categorization rule (right panel).

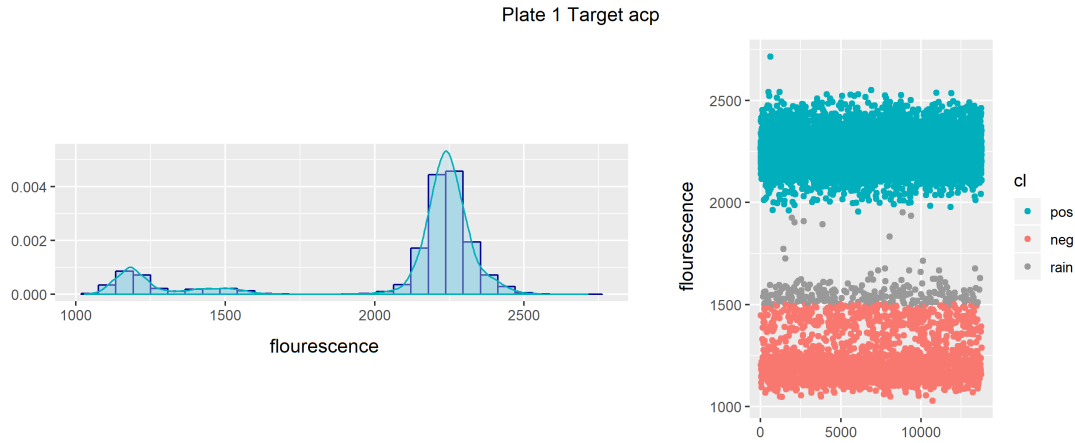


Figure 2.2: One replicate of the DNA target acp Plate 1 from Lievens et al. (2016) dataset. Left panel shows the fluorescence densities. Right panel is the result of droplet categorization using cloudy

It is noted that the context of the threshold setting here is based on in-house data for studying dPCR experiment optimization, and not necessarily as a classifier for external data. The constant threshold criterium enables the control for other PCR experimental factors, such as sonication, PCR enhancers, annealing conditions, and number of cycles, to achieve optimization or diminishing rain droplets for dPCR experiments.

#### 2.1.4 K-Nearest-Neighbors (KNN)

Based on the research papers curated by Peterson (2009), K-nearest-neighbor (KNN) is a unsupervised clustering approach that should be among the first methods considered for data with little to no information about its distribution. This clustering method operates on the chosen distance measure — commonly the Euclidean distance — between the observations. Due to its simplicity, data

from various fields have applied KNN such as in a movie recommendation system (Ahuja, Solanki, & Nayyar, 2019), climate classification (Shi & Yang, 2020), breast cancer diagnostics (Mittal, Aggarwal, & Mahajan, 2019), among others.

An open-source tool developed by Jones et al. (2014a), called *definetherain*, utilizes the KNN algorithm in identifying rain droplets. According to their research, they claim that *definetherain* is accurate in estimating assays with low template numbers, which is particularly applicable in research fields such as the HIV-1 cure research. *definetherain* follows these steps for classification:

1. Setup a positive control sample of known input copy numbers.
2. Cluster the droplets using kNN with  $k = 2$ . The cluster on the left is the negative cluster, and on the right is the positive cluster.
3. Observations between the range of the negative cluster's mean + 3 standard deviations and the positive cluster's mean - 3 standard deviations are classified as rain.
4. Rain droplets are not included in the final calculation of the concentration estimate.

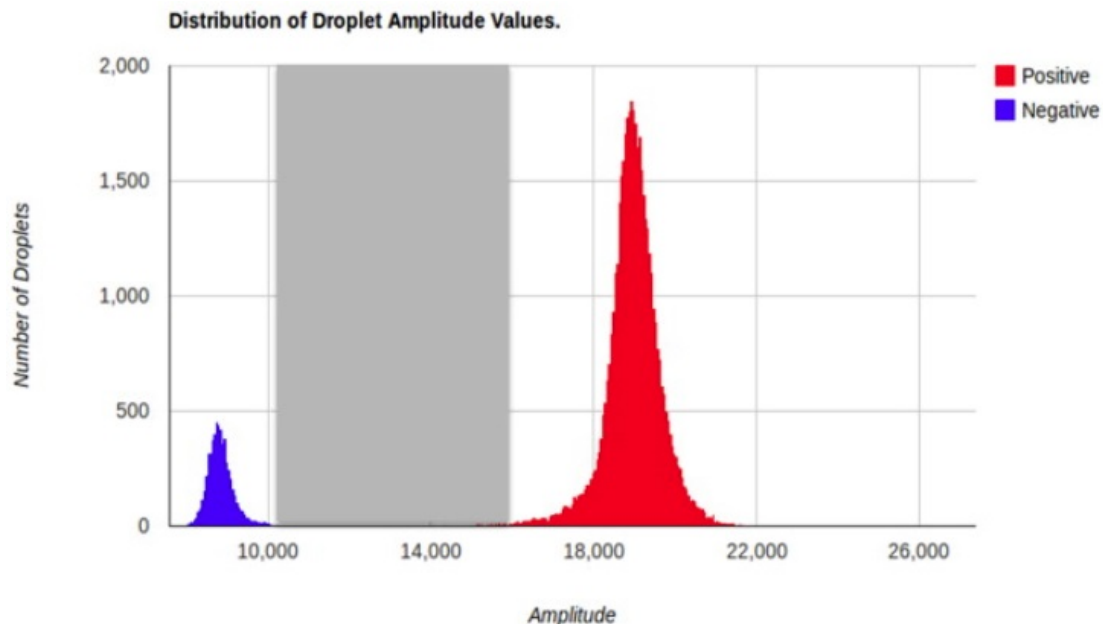


Figure 2.3: Determined thresholds calculated by *definetherain*, reprinted from (Jones et al., 2014b)

Unlike the other methods discussed here, this tool produces two cutoff values — one for each cluster. The droplets falling between these two values are classified as rain. These cutoff values are solely dependent on the control sample. The disadvantage of this is that the control has to be representative of the NA target; otherwise, concentration estimates would be biased.

### 2.1.5 Model-Based Clustering

As opposed to the distance-based clustering in Section 2.1.4, a probabilistic approach is achieved with model-based clustering. According to Mcnicholas (2016), in this approach, a cluster is defined as a unimodal component within a finite mixture model. The mixture model has to be appropriate in such that its parameters are flexible for fitting the characteristics of the data. Each observation, therefore, has a calculated probability of it belonging to a group. Using model-based clustering, studies have shown abstract data types with satisfactory outcomes. One example is image data in the study of (Choy, Lam, Yu, Lee, & Leung, 2017). They were able to perform image segmentation using the generalized Gaussian density model. Each cluster formed is interpreted as an object, and the number of which is identified via a validation technique. Their algorithm was able to segment objects such as a starfish, cat, or tree in photographs. Additionally, using genetic data, Li et al. (2018) discovered a potential differentially-variable microRNA (miRNA) not yet been reported in literature, upon fitting a three-component multivariate normal distribution to miRNA expression levels.

Jacobs et al. (2017) developed Umbrella, a model-based clustering for dPCR droplets available in source code (<https://github.com/statOmics/umbrella>). After providing a representative NTC sample(s), the procedure follows a series of estimation and assumptions in deriving the final estimated concentration. An oversimplification of the Umbrella procedure, that skips the detailed steps for handling specific cases, are as follows:

1. The NTC distribution  $f_0(x)$  is assumed to follow a unimodal distribution. The location and variation is estimated by the mode and mean of absolute deviation (MAD), respectively.
2. The fluorescence intensities  $x$  observed in partitions of a target partition set  $A$  is assumed to have a mixture density

$$f_A(x) = p_{0,A}f_{0,A}(x) + (1 - p_{0,A})f_{1,A}(x)$$

- $p_{0,A}$  = proportion of negative partitions

- $f_{0,A}(x)$  = densities of the partitions without target copy (null component of the target partition set  $A$ )
  - $(1 - p_{0,A})$  = proportion of positive partitions
  - $f_{1,A}(x)$  = densities of the partitions with target copy
3. Begin estimating the parameters by first aligning the modes of the null component of  $f_A(x)$  and the NTC reference  $f_0(x)$ .
  4. Discretize the aligned distributions by generating a histogram with the same bins.
  5. The bin counts of the aligned distribution are modeled using a Poisson regression model, resulting in estimates for  $\hat{p}_{0,A}$ ,  $\hat{f}_0(x)$ , and  $\hat{f}_A(x)$ .
  6. The posterior probability that partition  $i$  is void of the NA target with fluorescence intensity  $x_i$  of partition set  $A$ ,  $\hat{p}_{0,A}$ , can be defined from the estimated  $\hat{p}_{0,A}$  from the previous step as

$$\hat{p}_{i,0,A} = \hat{p}_{0,A} \left( \frac{\hat{f}_{0,A}(x_i)}{\hat{f}_A(x_i)} \right)$$

7. The Umbrella threshold estimator is then determined by the estimated  $\hat{p}_{i,0,A}$ . For intensity value  $i$ , the interpretation of the posterior probabilities are
  - $\hat{p}_{i,0,A} > 80\%$  are considered negative partitions with a probability of  $\leq 20\%$  to be false negatives
  - $\hat{p}_{i,0,A} < 5\%$  are considered positive partitions with a probability of  $\leq 5\%$  to be false positives
  - $5\% \leq \hat{p}_{i,0,A} \leq 80\%$  are considered as rain

The mode and MAD, as the location and spread estimators for the null NTC distribution,  $f_0(x)$ , are chosen due to its robustness and insensitivity to skewed tails. Only observations within 10 deviations of the mode are included for the null model.

Following the assumption of a mixture density in step 2, unlike most model-based clustering algorithms, Umbrella does not assume normal densities for  $f_{1,A}(x)$  and  $f_{0,A}(x)$ , the partitions with and without the NA target, respectively. This is due to the exhibition of dPCR fluorescence intensities to be non-normal, as clusters tend to have heavy tails to the left or to the right. The solution for this is the use of non-parametric density estimation in step 3.

After estimating all the components in the mixture model from steps 3 - 5, the component of interest  $p_{0,A}$  is then used to determine  $\hat{p}_{i,0,A}$  in step 6. Finally, this is used as the basis for Umbrella threshold estimator in step 7. It is cautioned that Umbrella may not be precise in detection experiments for low copy samples, as classifying individual samples is not the strength of this method.

## 2.2 Expectation-Maximization (EM) Clustering

# Chapter 3

## Theoretical Framework

### 3.1 EM Clustering

#### 3.1.1 Model-based clustering

#### 3.1.2 G-component Finite Mixture Density

#### 3.1.3 Expectation Maximization

### 3.2 Performance Evaluation



# Chapter 4

## Methodology

### 4.1 Data

#### 4.1.1 Rain Experiment Dataset

Plate 2 - Primer and Probe Concentration Gradient

Plate 4 - PCR Enhancers Experiment

Plate 5 - Cycle Gradient

Plate 6 - Sonication Gradient

Plate 7 - Annealing Temperature Gradient

#### 4.1.2 DNA Quantification Dataset

Plate 3 - Rain Dilution Series

Albumin

### 4.2 Model Fitting and Classification

### 4.3 Performance Evaluation



# Appendix A

## Diagrams and Other Documentation Tools

This appendix may consist of proposed architectural design, algorithms, scientific formula for MSCS and Data Flow Diagrams, Fishbone for MSIT.

## **Appendix B**

### **Theoretical and/or Conceptual Framework**

Discusses the basic framework/foundation the thesis is based on. This section is normally referred to when discussing Scope and Limitations, and Research Methodology

# Appendix C

## Resource Persons

**Dr. Firstname1 Lastname1**

Adviser

College of Computer Studies

De La Salle University-Manila

emailaddr@dlsu.edu.ph

**Mr. Firstname2 Lastname2**

Role2

Affiliation2

emailaddr2@domain.com

**Ms. Firstname3 Lastname3**

Role3

Affiliation3

emailaddr3@domain.net

# References

- Abed, Y., Carbonneau, J., L’Huillier, A. G., Kaiser, L., & Boivin, G. (2017). Droplet digital PCR to investigate quasi-species at codons 119 and 275 of the A(H1N1)pdm09 neuraminidase during zanamivir and oseltamivir therapies. *Journal of Medical Virology*, 89(4), 737–741. doi: 10.1002/jmv.24680
- Ahuja, R., Solanki, A., & Nayyar, A. (2019). Movie recommender system using k-means clustering and k-nearest neighbor. *Proceedings of the 9th International Conference On Cloud Computing, Data Science and Engineering, Confluence 2019*, 263–268. doi: 10.1109/CONFLUENCE.2019.8776969
- Basanisi, M. G., La Bella, G., Nobili, G., Coppola, R., Damato, A. M., Cafiero, M. A., & La Salandra, G. (2020). Application of the novel Droplet digital PCR technology for identification of meat species. *International Journal of Food Science and Technology*, 55(3), 1145–1150. doi: 10.1111/ijfs.14486
- Bio-Rad. (2019). *QX200™ Droplet Reader and QuantaSoft™ Software Instruction Manual*.
- Capobianco, J. A., Clark, M., Cariou, A., Leveau, A., Pierre, S., Fratamico, P., ... Armstrong, C. M. (2020). *Detection of Shiga toxin-producing Escherichia coli (STEC) in beef products using droplet digital PCR* (Vol. 319). Elsevier B.V. Retrieved from <https://doi.org/10.1016/j.ijfoodmicro.2019.108499> doi: 10.1016/j.ijfoodmicro.2019.108499
- Chen, D. F., Zhang, L. J., Tan, K., & Jing, Q. (2018). Application of droplet digital PCR in quantitative detection of the cell-free circulating circRNAs. *Biotechnology and Biotechnological Equipment*, 32(1), 116–123. Retrieved from <https://doi.org/10.1080/13102818.2017.1398596> doi: 10.1080/13102818.2017.1398596
- Chen, J., Zhang, Y., Chen, C., Zhang, Y., Zhou, W., & Sang, Y. (2020). Identification and quantification of cassava starch adulteration in different food starches by droplet digital PCR. *PLoS ONE*, 15(2), 1–16. Retrieved from <http://dx.doi.org/10.1371/journal.pone.0228624> doi: 10.1371/journal.pone.0228624
- Choy, S. K., Lam, S. Y., Yu, K. W., Lee, W. Y., & Leung, K. T. (2017). Fuzzy model-based clustering and its application in image segmentation. *Pattern*

- Recognition*, 68, 141–157. Retrieved from <http://dx.doi.org/10.1016/j.patcog.2017.03.009> doi: 10.1016/j.patcog.2017.03.009
- Dobnik, D., Štebih, D., Blejec, A., Morisset, D., & Žel, J. (2016). Multiplex quantification of four DNA targets in one reaction with Bio-Rad droplet digital PCR system for GMO detection. *Scientific Reports*, 6(September), 1–9. doi: 10.1038/srep35451
- Dreo, T., Pirc, M., Ramšak, Ž., Pavšič, J., Milavec, M., Žel, J., & Gruden, K. (2014). Optimising droplet digital PCR analysis approaches for detection and quantification of bacteria: A case study of fire blight and potato brown rot. *Analytical and Bioanalytical Chemistry*, 406(26), 6513–6528. doi: 10.1007/s00216-014-8084-1
- Hamaguchi, M., Shimabukuro, H., Hori, M., Yoshida, G., Terada, T., & Miyajima, T. (2018). Quantitative real-time polymerase chain reaction (PCR) and droplet digital PCR duplex assays for detecting *Zostera marina* DNA in coastal sediments. *Limnology and Oceanography: Methods*, 16(4), 253–264. doi: 10.1002/lom3.10242
- Hinneburg, A., & Keim, D. A. (2003). A General Approach to Clustering in Large Databases with Noise. *Knowledge and Information Systems*, 5(4), 387–415. doi: 10.1007/s10115-003-0086-9
- Huggett, J. F., O’Grady, J., & Bustin, S. (2015). QPCR, dPCR, NGS - A journey. *Biomolecular Detection and Quantification*, 3(March 2007), A1–A5. doi: 10.1016/j.bdq.2015.01.001
- Hussain, M., & Bowers, J. (2017a). A Droplet Digital PCR Method for CHO Host Residual DNA Quantification in Biologic Drugs. *Journal of Analytical & Pharmaceutical Research*, 4(3), 8–11. doi: 10.15406/japlr.2017.04.00107
- Hussain, M., & Bowers, J. (2017b). A droplet digital pcr method for cho host residual dna quantification in biologic drugs - scientific figure on researchgate. Retrieved from [https://www.researchgate.net/figure/Droplet-fluorescence-amplitude-with-CHO-hrDNA-ddPCR-method-The-mAb-DS4P-52g-was\\_fig1\\_316088304](https://www.researchgate.net/figure/Droplet-fluorescence-amplitude-with-CHO-hrDNA-ddPCR-method-The-mAb-DS4P-52g-was_fig1_316088304) ([Online; accessed April 7, 2020])
- Jacobs, B. K., Goetghebeur, E., & Clement, L. (2014). Impact of variance components on reliability of absolute quantification using digital PCR. *BMC Bioinformatics*, 15(1), 1–13. doi: 10.1186/1471-2105-15-283
- Jacobs, B. K., Goetghebeur, E., Vandesompele, J., De Ganck, A., Nijs, N., Beckers, A., ... Clement, L. (2017). Model-Based Classification for Digital PCR: Your Umbrella for Rain. *Analytical Chemistry*, 89(8), 4461–4467. doi: 10.1021/acs.analchem.6b04208
- Jahne, M. A., Brinkman, N. E., Keely, S. P., Zimmerman, B. D., Wheaton, E. A., & Garland, J. L. (2020). Droplet digital PCR quantification of norovirus and adenovirus in decentralized wastewater and graywater collections: Implications for onsite reuse. *Water Research*, 169, 115213. Retrieved from <https://doi.org/10.1016/j.watres.2019.115213> doi:

- 10.1016/j.watres.2019.115213
- Jones, M., Williams, J., Gärtner, K., Phillips, R., Hurst, J., & Frater, J. (2014a). Low copy target detection by Droplet Digital PCR through application of a novel open access bioinformatic pipeline, 'definetherain'. *Journal of Virological Methods*, 202, 46–53. Retrieved from <http://dx.doi.org/10.1016/j.jviromet.2014.02.020> doi: 10.1016/j.jviromet.2014.02.020
- Jones, M., Williams, J., Gärtner, K., Phillips, R., Hurst, J., & Frater, J. (2014b). *Low copy target detection by Droplet Digital PCR through application of a novel open access bioinformatic pipeline, 'definetherain'*. Retrieved from [https://www.researchgate.net/figure/Screenshots-illustrating-the-application-of-definetherain-Screenshots-illustrating-the\\_fig2\\_260441031](https://www.researchgate.net/figure/Screenshots-illustrating-the-application-of-definetherain-Screenshots-illustrating-the_fig2_260441031) ([Online; accessed April 7, 2020])
- Junior, F. C., Da Silva, T. L., De Queiroz Neto, J. F., De MacÊdo, J. A. F., & Porcino, W. C. (2019). A novel approach to approximate crime hotspots to the road network. *Proceedings of the 3rd ACM SIGSPATIAL International Workshop on Prediction of Human Mobility, PredictGIS 2019*, 53–61. doi: 10.1145/3356995.3364538
- Kauhl, B., Schweikart, J., Krafft, T., Keste, A., & Moskwyn, M. (2016). Do the risk factors for type 2 diabetes mellitus vary by location? A spatial analysis of health insurance claims in Northeastern Germany using kernel density estimation and geographically weighted regression. *International Journal of Health Geographics*, 15(1), 1–12. doi: 10.1186/s12942-016-0068-2
- Li, X., Fu, Y., Wang, X., Demeo, D. L., Tantisira, K., Weiss, S. T., & Qiu, W. (2018). Detecting Differentially Variable MicroRNAs via Model-Based Clustering. *International Journal of Genomics*, 2018. doi: 10.1155/2018/6591634
- Lievens, A., Jacchia, S., Kagkli, D., Savini, C., & Querci, M. (2016). Measuring Digital PCR Quality: Performance Parameters and Their Optimization. *PloS one*, 11(5), e0153317. doi: 10.1371/journal.pone.0153317
- López, S. O., García-Olmo, D. C., García-Arranz, M., Guadalajara, H., Pastor, C., & García-Olmo, D. (2016). KRAS G12V mutation detection by droplet digital PCR in circulating cell-free DNA of colorectal cancer patients. *International Journal of Molecular Sciences*, 17(4), 1–9. doi: 10.3390/ijms17040484
- Mauvisseau, Q., Davy-Bowker, J., Bulling, M., Brys, R., Neyrinck, S., Troth, C., & Sweet, M. (2019). Combining ddPCR and environmental DNA to improve detection capabilities of a critically endangered freshwater invertebrate. *Scientific Reports*, 9(1), 1–9. Retrieved from <http://dx.doi.org/10.1038/s41598-019-50571-9> doi: 10.1038/s41598-019-50571-9
- McNicholas, P. D. (2016). Model-Based Clustering. , 373(November), 331–373. doi: 10.1007/s0035

- Mehmood, R., Zhang, G., Bie, R., Dawood, H., & Ahmad, H. (2016). Clustering by fast search and find of density peaks via heat diffusion. *Neurocomputing*, 208, 210–217. Retrieved from <http://dx.doi.org/10.1016/j.neucom.2016.01.102> doi: 10.1016/j.neucom.2016.01.102
- Mittal, K., Aggarwal, G., & Mahajan, P. (2019). Performance study of K-nearest neighbor classifier and K-means clustering for predicting the diagnostic accuracy. *International Journal of Information Technology*, 11(3), 535–540. Retrieved from <https://doi.org/10.1007/s41870-018-0233-x> doi: 10.1007/s41870-018-0233-x
- Nystrand, C. F., Ghanima, W., Waage, A., & Jonassen, C. M. (2018). JAK2 V617F mutation can be reliably detected in serum using droplet digital PCR. *International Journal of Laboratory Hematology*, 40(2), 181–186. doi: 10.1111/ijlh.12762
- Peterson, L. E. (2009). K-nearest neighbor. *Scholarpedia*, 4(2), 1883. (revision #137311) doi: 10.4249/scholarpedia.1883
- Quan, P. L., Sauzade, M., & Brouzes, E. (2018). DPCR: A technology review. *Sensors (Switzerland)*, 18(4). doi: 10.3390/s18041271
- Rodriguez, A., & Laio, A. (2014). Clustering by fast search and find of density peaks. *Science*, 344(6191), 1492–1496. doi: 10.1126/science.1242072
- Shi, J., & Yang, L. (2020). A climate classification of China through k-nearest-neighbor and sparse subspace representation. *Journal of Climate*, 33(1), 243–262. doi: 10.1175/JCLI-D-18-0718.1
- Stopka, T. J., Goulart, M. A., Meyers, D. J., Hutcheson, M., Barton, K., Onofrey, S., ... Chui, K. K. (2017). Identifying and characterizing hepatitis C virus hotspots in Massachusetts: A spatial epidemiological approach. *BMC Infectious Diseases*, 17(1), 1–11. doi: 10.1186/s12879-017-2400-2
- Tagliapietra, A., Rotondo, J. C., Bononi, I., Mazzoni, E., Magagnoli, F., Gonzalez, L. O., ... Martini, F. (2020). Droplet-digital PCR assay to detect Merkel cell polyomavirus sequences in chorionic villi from spontaneous abortion affected females. *Journal of Cellular Physiology*, 235(3), 1888–1894. doi: 10.1002/jcp.29213
- Tzonev, S. (n.d.). Chapter 3 Fundamentals of Counting Statistics in Digital PCR : I Just. , 1768, 25–43.
- Wang, S., Wang, D., Li, C., Li, Y., & Ding, G. (2016). Clustering by fast search and find of density peaks with data field. *Chinese Journal of Electronics*, 25(3), 397–402. doi: 10.1049/cje.2016.05.001
- Whale, A. S., Cowen, S., Foy, C. A., & Huggett, J. F. (2013). Methods for Applying Accurate Digital PCR Analysis on Low Copy DNA Samples. *PLoS ONE*, 8(3). doi: 10.1371/journal.pone.0058177
- Zang, W., Ren, L., Zhang, W., & Liu, X. (2017). Automatic Density Peaks Clustering Using DNA Genetic Algorithm Optimized Data Field and Gaussian Process. *International Journal of Pattern Recognition and Artificial*

*Intelligence*, 31(8), 1–28. doi: 10.1142/S0218001417500239